AN ELUCIDATION ON ADHESIVE STRENGTH OF AL 2 O 3 AND ZRO 2 5CAO COMPOSITE COATINGS APPLIED ON AL-6061 & CI SUBSTRATES

Experiment Findings · June 2018

DOI: 10.13140/RG.2.2.17125.45281

CITATIONS
0

READS
124

5 authors, including:

Abhinav
Dayananda Sagar Academy of Technology and Management
25 PUBLICATIONS **33** CITATIONS
SEE PROFILE

N. Krishnamurthy
vijaya vittala institute of technology
15 PUBLICATIONS **136** CITATIONS
SEE PROFILE

Ranjana Jain
8 PUBLICATIONS **22** CITATIONS
SEE PROFILE

International Journal of Mechanical and Production Engineering Research and Development (IJMPERD)
ISSN (P): 2249-6890; ISSN (E): 2249-8001
Special Issue, Jun 2018, 91-98

TRANS STELLAR
•Journal Publications •Research Consultancy

AN ELUCIDATION ON ADHESIVE STRENGTH OF AL_2O_3 AND $ZRO_2$5CAO COMPOSITE COATINGS APPLIED ON AL-6061 & CI SUBSTRATES

ABHINAV[1], N. KRISHNAMURTHY[2], RANJANA JAIN[3] & PHV SESHA TALPASAI[4]

[1]*Department of Mechanical Engineering, Alliance University, Bangalore, India*

[2]*Department of Mechanical Engineering, Vijaya Vittala Institute of Technology, Bangalore, India*

[3]*Department of Chemistry, Kammavari Sangha Institute of Technology, Bangalore, India*

[4]*Department of Mechanical Engineering MRCET, Hyderabad, India*

ABSTRACT

In this study, the adhesion strength of atmospheric plasma sprayed coatings on cast iron and Al-6061substrates were carried out. Alumina and calcia stabilized zirconia in 50:50 proportion by weight were blended in a ball mill and applied as a top coat. The top coat thickness was varied as 100 µm, 200 µm, and 300µm. Adhesion test was conducted as per ASTM C633 standard and a comparative analysis was done. SEM micrographs revealed that the weakest link was formed between the top coat/bond coat interfaces in all the coating systems. Relatively higher adhesion strength was found due to the excellent metallurgical bonding between Al_2O_3-ZrO_2·5CaO topcoat and Ni-Al bond coat in the case of the cast iron 300µm coating system. An attempt has been made to bring out an insight into the principal causes of adhesion failure for the above coating combinations.

KEYWORDS: Plasma Sprayed Coatings, Thermal Barrier Coatings, Microstructure, Adhesion Strength

Original Article

INTRODUCTION

Several studies have been explored to determine the behaviour and performance of ceramic coatings on metal substrates [1-4]. The applications are (but not limited to) cutting tools [1], high temperature parts of engines [2], gas turbine components [3], and bone joint prostheses [5]. The advantages of such coatings are improved corrosion resistance, high temperature resistance, good wear resistance, high hardness, good tribological characteristics and good biocompatibility. Adhesion strength is a preliminary requirement for any Thermal Barrier Coating (TBC). Several mechanisms of adhesion possible are: mechanical keying, physical, diffusive or chemical [6,7]. Many studies have been carried out to determine the adhesion strength of ceramic coatings. It is found that surface roughness, porosity, thickness of the coating, co-adherence of the splats and splat morphology, substrate-coating composition, environmental conditions, curing process are the key parameters that influence the adhesion strength of the coatings [8]. The adhesion strength also profoundly depended on surface preparation techniques, which includes cleaning, heating, blasting etc. [9]. It has been reported that thin films of adhesive in the range of 50-1000 nm formed between the bond coat and top coat affect the adhesion strength of TBC coatings. Its effect on coating is still a debatable area and not yet clearly explained [10,11]. The tensile test is well accepted in the determination of adhesion strength and also resistance against shearing load [12,13]. It is widely understood that hardness increases with increase in local particle density and at the same time decreases with number of pores and micro-cracks [14]. In the graded coating system, the top coat and bond coat provides a thermal history of the top coat [14, 15]. The ASTM C633 [16] standard test is a well-accepted technique for evaluating the adhesion strength.

In this test, the coated sample is glued to another similarly coated counterpart and then tested in tension in a universal testing machine. Krishnamurthy et al. [17] have conducted adhesion tests on two types of powder, ZrO_2.5CaO and Al_2O_3 powders of different coating thicknesses and validated successfully.

In the present investigation, an attempt has been made to determine the adhesive strength/tensile strength of the coating systems applied on Al-6061 and Cast iron(CI) substrates using the atmospheric plasma spray technique. The surface morphology, microhardness, porosity, surface roughness and adhesion strength were evaluated and also the main reason for coating failure has been discussed in detail.

EXPERIMENTAL DETAILS

Selection of Materials and Coating Compositions

The elemental compositions of Al-6061 and CI are mentioned in Tables 1 and 2 respectively. The trade names and composition of the powder materials for coating are provided in table 3.

Table 1: Al-6061 Substrate Elemental Composition

Element	Si	Fe	Cu	Mn	Mg	Zn	Cr	Ti	Others
Weight %	0.60	0.75	0.16	0.15	0.64	0.25	0.03	0.03	0.12

Table 2: Cast Iron Substrate Elemental Compositions

Element	C	Si	Mn	Cr	Cu	P	S	Ni
Weight %	3.854	1.91	0.04	0.03	0.02	0.082	0.097	<0.05

Table 3: Trade Name and Composition of the Powder

Trade Name	Composition by wt.%
Metco 105 SFP Metco 201 NS(top coat)	99.9% Al_2O_3 ZrO_2.5CaO
Metco 452 (bond coat for ci)	Fe38Ni10Al
Metco 446 (bond coat for Al-6061)	Al25Fe7Cr5Ni
Metco 410 NS (bond coat for Al-6061)	$Al_2O_3$30(Ni20Al)

Coating Methodology

The atmospheric plasma spraying technique was adopted to coat the substrates. Before the coating process, the mixture of Al_2O_3 and ZrO_2.5CaO in 50:50 percentages by weight was prepared using the ball mill technique. Initially, the substrates were chemically cleaned using tetra chloride-ethylene followed by preheating treatment to a temperature of approximately 300±50 ºC to ensure good adhesion strength between the substrate and bond coat. The schematic of coating systems for Al-6061 and CI are shown in Figure 1 and 2 respectively. The plasma spray parameters for bond coat and top coat are given in Table 4. The coated plates and cylindrical specimens are shown in Figure 3. Cylindrical specimens of diameter 25mm and length 80mm (Figure 4) were used for the adhesion tests. Plates of dimensions 1cm x 1cm were selected for micro hardness and roughness tests.

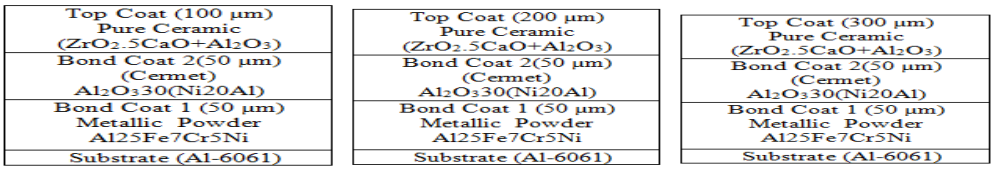

Figure 1: Schematic diagram of the Coating Systems on Al-6061 Substrate

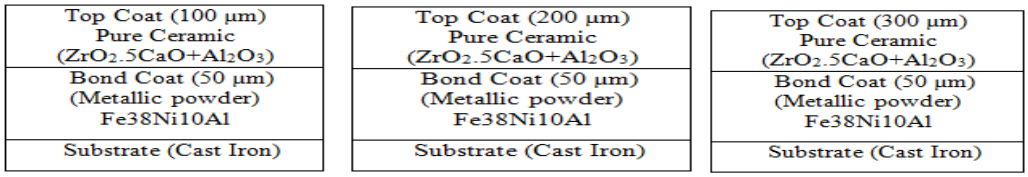

Figure 2: Schematic diagram of Cast Iron Coating System

Table 4: Plasma Spray Parameters for Different Coating Materials

Materials	Primary Gas (Argon) Pressure(Bar)	Secondary Gas (Hydrogen) Pressure (Bar)	Carrier Gas Argon Flow (LPM)	Current (Amps)	Voltage (Volts)	Spray Distance (mm)
Al_2O_3+ ZrO_2.5CaO	3.7	3.45	35	500	65	65-76
Fe38Ni10Al	6.9	3.30	35	500	65	50-76
Al25Fe7Cr5Ni	6.9	3.30	35	500	65	50-76
$Al_2O_3$30(Ni20Al)	3.7	3.45	35	500	65	65-76

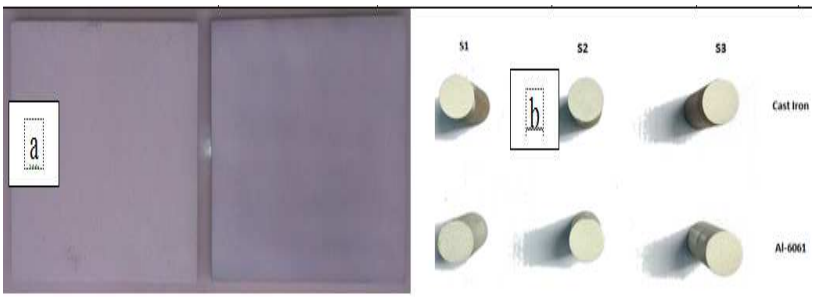

Figure 3(a): Coated Plates and b. Coated Cylindrical Specimens

Determination of Micro Hardness and Porosity

The measurement of micro hardness and porosity of the coatings were done as per ASTM E384 standard [18] and line intercepts technique respectively. A sample size of 10 × 10 mm cut from the plates and cross-sections were subjected to polishing and buffing. The micro hardness was measured by Vickers hardness tester under 100g load using CMT. HD model. An average of five readings was recorded at different locations on the top coat and at the interfaces of the coating system.

Determination of Surface Texture and Morphology of the Coating

The surface texture of the coated samples was examined using a Mitutoyo SJ-210 surface roughness tester as per ISO1997 standard. The probe traveling speed was maintained at 0.5mm/s. Other important specifications of the device are as follows: stylus tip radius 5µm, detecting measuring force 4mN, and display-LCD. Morphology of the coatings was examined using a Zeiss Evo 18 special edition machine. The machine specifications are given in Table 5. Backscattered electron techniques were adapted to study the surface morphology of the top coat.

Table 5: SEM Machine Specifications

Materials	Primary Gas (Argon) Pressure(Bar)	Secondary Gas (Hydrogen) Pressure (Bar)	Carrier Gas Argon flow (LPM)	Current (Amps)	Voltage (Volts)	Spray Distance (mm)
Al_2O_3+ ZrO_2.5CaO	3.7	3.45	35	500	65	65-76
Fe38Ni10Al	6.9	3.30	35	500	65	50-76
Al25Fe7Cr5Ni	6.9	3.30	35	500	65	50-76
$Al_2O_3$30(Ni20Al)	3.7	3.45	35	500	65	65-76

Adhesion Test

The adhesion test was carried out as per ASTM C633 standard. For the test, nine coated cylindrical specimens were developed in a pair each for Al-6061 and CI. The dimensions of specimens are shown in Figure 4. The coated cylindrical specimens were joined using Epoxy polymer EP15 with the following specifications (Tensile strength > 84 MPa, Viscosity at 75°F, cps = 90000–100000) and cured in a muffle furnace. The temperature of the furnace was maintained at 180±5 ºC for 1 hour and the specimens were taken out and cooled at atmospheric temperature. The specimens were tested in a universal testing machine (UTM – Asian make, 60 ton capacity). The schematic of the experimental setup is shown in Figure 5. A digital indicator connected with a UTM gradually recorded the applied load and tensile stresses were calculated based on the circular cross-sectional area. On each sample, 3 trials were done and the average value was taken. The average values of the adhesion test are shown in Table 6.

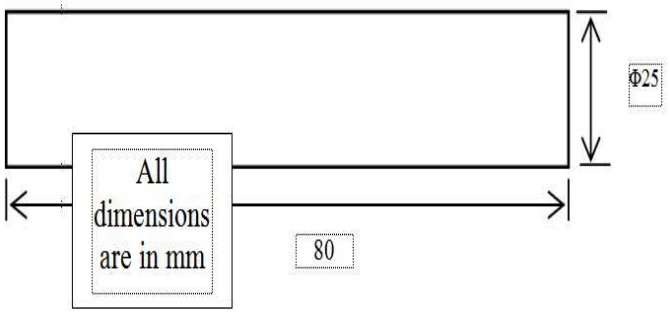

Figure 4: Dimensions of the Cylindrical Specimens

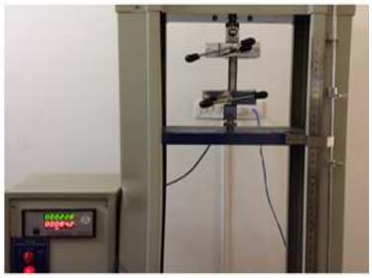

Figure 5: Universal Testing Machine with Adhesion Test Samples

RESULTS AND DISCUSSIONS

Figure 6 shows the fractured surfaces of adhesion test specimens.

From the Figure, it is noticed that the location of the coating failure in Al-S1 is at the interface between bond coat and substrate. This type of failure is termed as adhesion failure. In the remaining samples, incomplete fracture has been noticed. These samples probably could have higher value of adhesion strength. The mean value of bond strength of samples Al-S1, Al-S2 and Al-S3 are 20.2, 21.4 and 19.5MPa respectively. In case of CI-S1, CI-S2 and CI-S3, it is about 38.5, 43.56 and 49.3MPa respectively. The samples which undergone failure at topcoat/cermet interface indicates that pure ceramic has less affinity towards cermet and with the intermetallic bond coat. It is evident from the SEM micrograph of AlS1, AlS2 & AlS3 coating systems (Figure 8), the top coat is not able to establish good metallurgical bonding with the cermet bond coat, the reason attributed to a large thermal mismatch between the constituents of pure ceramic with cermet and has been confirmed with the microcracks at the interfaces (Figure 7). The microcracks formed in the topcoat also affect

the bond as crack propagation usually perpendicular to the applied load and is generally trans-granular, along cleavage planes. These kinds of flaws are very difficult to control in the manufacturing process and often leads to large variability in the adhesion strength or fracture strength of the pure ceramic material [19]. The thermal mismatch is more pronounced in case of Al-S3 coating system as it gives lesser bond strength compared to Al-S1 and Al-S2. This may be attributed to the occurrence of residual stresses between the top coat and bond coat which is often termed as free-edge-effect, as reported by E. F. Rybicki et al. [20]. Apart from thermal mismatch, microvoids play a crucial role in the determination of adhesion strength. It is also found that the porosity is relatively more in case of Al-6061 compare to CI coating systems. This could also be a probable reason of less adhesion strength in Al-6061 substrate samples compared to CI substrate coating samples.

In case of the CI substrate coating systems, very good metallurgical bonding was built between the substrate and bond coats as these systems shows no thermal distortion and the coating did not spell out from the substrate in any of the coating systems. The maximum tensile strength/adhesion strength was found to be 49.3MPa in the case of the CI-S3 sample. It is also understood that as the coating thickness increased, the adhesion strength also increased in both the coating systems. In the context of coating thickness, it is also revealed that the micro hardness of the top coat strongly depends on the porosity of the coatings and coating morphology. As the coating thickness increased, the micro hardness also increased. The shape of the coating splats and roughness of the top coat also play a pivotal role in deciding the adhesion strength of the coating [21]. The flattened splats in the case of the CI coating system was found to promote better adhesion and was may be a reason for higher tensile strength compared to Al-6061 coating systems (Figure 8). The morphology of the top coat for both the coating systems was determined and found that uneven granular deposits, pinholes, agglomeration, promoted high surface roughness in the case of Al-6061 coating systems (Figure 8). On the other hand, the CI coating systems exhibited more or less uniformly distributed splats and exhibited comparatively less surface roughness.

The average surface roughness, average micro hardness, average porosity and average adhesion strength of the individual coating system is shown in Table 6.

The material composition of the individual composite powders of the topcoat and bond coats, along with the coating process has influenced the adhesive strength of the coatings. It is evident from the SEM micrograph that topcoat composition of Al_2O_3-ZrO_2·5CaO in 50:50 wt. % makes good adhesion with the metallic bond coat Fe38Ni10Al in the case of the CI substrate. However, 70 wt. % of Al_2O_3 along with 30wt. % of Nickel-Aluminide cermet composition was not able to develop proper mechanical interlocking with the ceramic composition owing to the large difference in coefficient of thermal expansion. A number of research investigations have been conducted on Ni-Al based alloys [22] and are also found in commercial applications [23]. Low adhesion strength in the case of Al-6061 compared to CI coating systems in this experimental study attributed to less surface roughness value and the similar reason found and mentioned by Krishnamurthy et al. [17]. Over all, very good mechanical keying was observed between substrates and bond coat in the case of CI compared to Al-6061 coating systems.

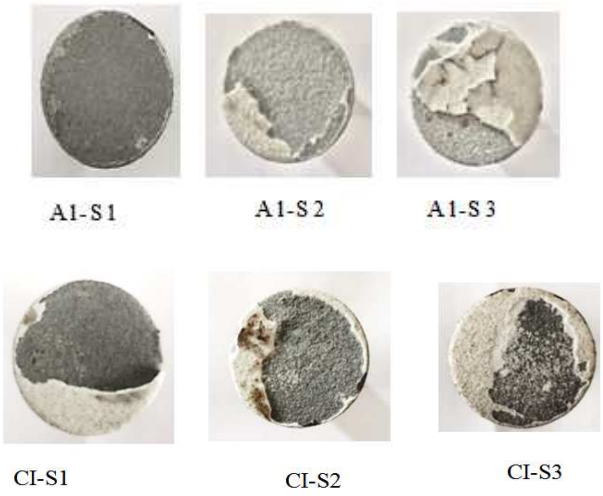

Figure 6: Fractured Surfaces of Adhesion Test Specimens

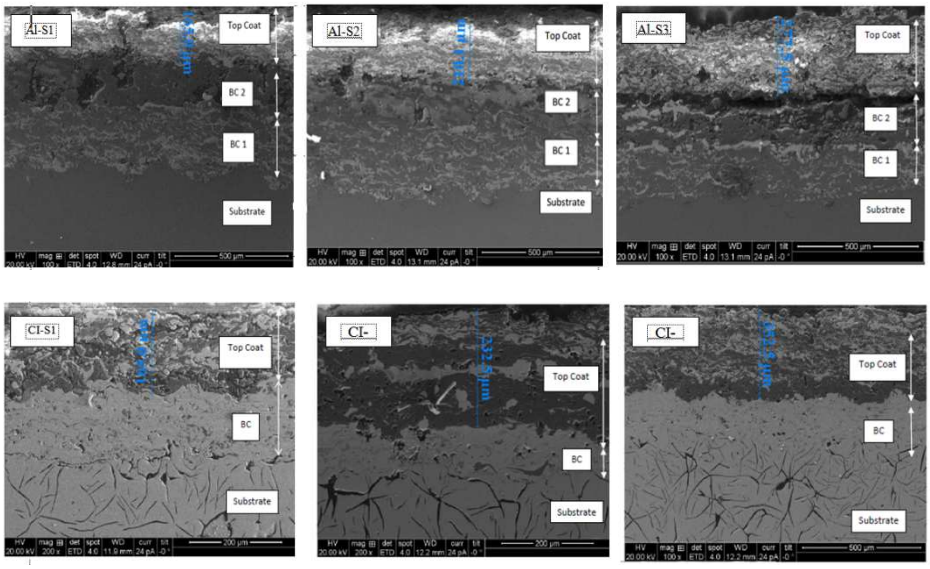

Figure 7: SEM Cross-Sections Views of Al-6061 CI Substrate Coating Systems

Table 6: Surface Roughness, Hardness, Porosity & Adhesion Strength Values of Coating Systems

Sample	Aluminium Substrate			Cast Iron Substrate		
	S1	S2	S3	S1	S2	S3
Surface Roughness (µm)	5.90	6.74	7.278	5.432	5.975	6.376
Hardness ($HV_{0.1}$)	442.21	585	616.8	556.42	668.98	708.03
Porosity(%)	1.58	1.41	1.0	1.9	1.71	1.52
Adhesion Strength (MPa)	5.40	5.56	5.03	6.40	6.77	9.33
Note: All the above data is an average value taken after number of trials						

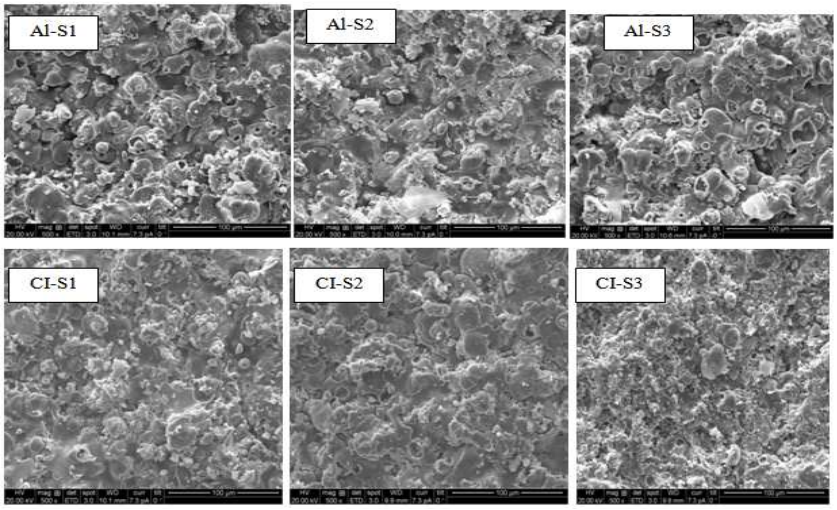

Figure 9: SEM Morphology of Al-6061 and CI Substrate Coating Systems

CONCLUSIONS

Judicious selection of bond coat composition along with topcoat powder is a preliminary requirement for good bond strength. The thermal coefficient of expansion of individual elements, surface roughness, and morphology were found to be key parameters in deciding the adhesion strength of the materials. SEM micrographs of the coating adhesion between Al_2O_3-ZrO_2·5CaO with Ni-Al intermetallic bond coat exhibited good mechanical interlocking. Also flattened splats of grains promoted better adhesion and the same was supported by the less surface roughness values in the case of CI compared to the Al-6061 coating system. It can be also concluded that adhesion strength profoundly depends upon the sum of the contact areas of mating surface asperities and the structure of the coating splats.

REFERENCES

1. *Attar, F., Johannesson, T., 1996, Surface and Coatings Technology 78, pp. 87-102.*
2. *Schulz, U., Leyens, C., Fritscher, K., Peters, M., Saruhan-Brings, B., Lavigne, O., Dorvaux, J., 2003, Aerospace Science and Technology 7(1), pp. 73-80.*
3. *Stern, K. H., 1996, Metall. and Ceramic Protective Coatings, Chapman & Hall, London, U. K., pp. 342.*
4. *Perumal, G., Geetha, M., Asokamani, R., Alagumurthi, N., 2014, Wear 31, pp. 101-113.*
5. *Ribeiro, R., Ingole, S., Usta, M., Bindal, C., Ucisik, A. H., Liang, H., 2007, Wear 262, pp. 1380-1386.*
6. *AWS, 1985, Thermal Spraying-Practice, Theory and Application. Miami FL: American Welding Society, 188pp.*
7. *Sobolev, V. V., Guilemany J. M., Nutting J., Miguel J. R., 1997, International Materials Reviews, 42(3), pp. 117-136. DOI: 10.1179/imr.1997.42.3.117*
8. *Meine, K., Klob, K., Schneider, T., Spaltmann, D., 2004, "The influence of surface roughness on the adhesion force," Surface and Interface Analysis 36(8), pp. 694-697.*
9. *Wegman, R. F., Twisk, J. V., 2012, Surface Preparation Techniques for Adhesive Bonding, Elsevier, New York, 168pp.*
10. *Harmsworth, P. D., Stevens, R., 1992, "Microstructure of zirconia-yttria plasma-sprayed thermal barrier coatings," Journal of Materials Science 27(3), pp. 616-624.*

11. *Bartuli, C., Bertamini, L., Matera, S., Sturlese, S., 1995, "Investigation of the formation of an amorphous film at the ZrO_2-Y_2O_3/NiCoCrAlY interface of thermal barrier coatings produced by plasma spraying," Materials Science and Engineering: A, 199(2), pp. 229-237.*
12. *Era H., Otsubo F., Uchida T, Fukudab S., Kishitake K., 1998, "A modified shear test for adhesion evaluation of thermally sprayed coating," Materials Science and Engineering 251(1-2), pp. 166-172.*
13. *Zhu Y. L., Ma S. N., Xu, B. S., Journal of Thermal Spray Technology 8(2), 1999, pp. 328–332.*
14. *Janos B. Z., Lugscheider E., Remer P. Surface and Coatings Technology, 113(3), 1999, pp. 278–285.*
15. *Haynes J. A., Ferber M. K, Porter, 1999, Materials at High Temperatures, 16(2), pp. 49–69.*
16. *ASTM. Standard test method for adhesion and cohesion strength of thermal spray coating. ASTM standard C-633-01, West Conshohocken, PA, USA: ASTM International, 2001.*
17. *Krishnamurthy, N., Sharma, S. C., Murali, M. S., Mukunda, G., Frontiers of Materials Science in China, 3(3), 2009, pp. 333–338.*
18. *ASTM Standard test method for micro-indentation hardness of materials. ASTM E384. West Conshohocken, PA, USA: ASTM International, 2005.*
19. *Dowling, N. E., 1993, Mechanical Behavior of Materials, Fourth Edition, Pearson Education Limited.*
20. *Rybicki, E. E., Schmuesser, D. W. Journal of Composite Materials, 12(3), 1978, pp. 300-313.*
21. *Yang, K., Liu, M., Zhou, K., Deng, C., 2013, Hindawi Publishing, Journal of Materials Vol.2013*
22. *National Materials Advisory Board. Intermetallic Alloy Development; NMAB-487-1; National Academy Press: Washington, DC, USA, 1997.*
23. *Varin, R. A.; Martin, J., Ed.; Elsevier: Amsterdam, The Netherlands, 2007, pp. 235–238.*